

## Local activation of light-induced degradation in co-doped boron-phosphorus silicon: Evidence of defect diffusion phenomena

M. Najjar <sup>a,b</sup>, B. Dridi Rezgui <sup>a</sup>, M. Bouaicha <sup>a</sup>, O. Palais <sup>c</sup>, B. Bessais <sup>a</sup>, S. Aouida <sup>a,\*</sup>

<sup>a</sup> Laboratoire de Photovoltaïque, Centre de Recherches et des Technologies de l'Energie, Technopôle de Borj-Cédria, Hammam-Lif, 2050, BP 95, Tunis, Tunisia

<sup>b</sup> University of Tunis, Higher National Engineering School of Tunis (ENSIIT), Tunis, 1008, Tunisia

<sup>c</sup> Aix Marseille Université, Université de Toulon, CNRS, IM2NP, 13397, Marseille, France



### ARTICLE INFO

#### Keywords:

Silicon solar cell

Light induced degradation

Carrier lifetime

### ABSTRACT

This study is interested in the local activation of Light-induced degradation (LID) defect in highly co-doped silicon wafers with boron and phosphorus. For this purpose, the experiments are focused on measuring the minority carrier lifetime before and after LID activation via a mapping technique. The LID defect density exhibits a Gaussian distribution centered on the excitation point of the laser beam; the intensity of the Gaussian distribution of the LID defect varies with the concentration of the co-dopants. The lifetime of the minority carriers decreases in all-silicon sample regions, while the excitation laser beam focuses on an area of approximately one mm<sup>2</sup>. This observation indicates that LID defects are activated even in the unexcited areas of silicon wafers, suggesting a LID diffusion phenomenon from the laser excitation point to the whole silicon wafer. We deduce that a high phosphorus doping level in silicon wafers leads to a significant reduction in the LID effect.

### 1. Introduction

Light-induced degradation (LID) has received considerable attention in recent years due to its detrimental impact on the performance of photovoltaic (PV) solar cells under field conditions [1]. Several studies investigating this effect have been published and introduced various trends and interpretations [2–16]. The LID phenomenon was firstly presented in 1973 by Fischer and Pschunder [2]; they observed a significant degradation of the efficiency of Cz-based silicon solar cells under illumination. After a few hours of illumination, the degradation stops—furthermore, a heat treatment at a low temperature around 200 °C regenerates the initial state. Measurements of the decrease in photoconductance have shown that the observed degradation is due to a decrease in the lifetime of minority carriers of the solar cell base material. The minority carrier lifetime balances between two levels. High and low values after low-temperature treatment and illumination, respectively [2,5]. The carrier lifetime variation was attributed to the activation/annihilation of electrically active defects. Since this observation, various models and interpretations have been proposed to explain the origin of these defects. Later in 1979, Weizer et al. [17] reported photo degradation in n<sup>+</sup>/p silicon solar cells under illumination at open circuit operation and under illumination with specific

wavelength at short circuit operation [17]. The spectral response of the cells shows that the recombination centers (responsible for the minority carrier decrease) are located in the base (p-type region) region of the solar cell and not in the diffused region (n<sup>+</sup>-type region) [17]. In a first interpretation, Weizer et al. associated the activated recombination centers with defect pairs formed by a lattice defect and silver atom or complex of atoms introduced in the cell-contact metallization step. This assumption is weak because the minority carrier lifetime also decreases under illumination in a passivated silicon wafer. Corbett et al. [18] indicated light illumination of boron-doped silicon wafer active various defect pairs; they reported more than 50 possible reactions for defect formation. Several years later, Knobloch et al. [3] reported that the presence of excess minority carriers causes the degradation in boron-doped silicon and not photons. Glunz et al. [19] and Hashigami et al. [7] confirm this result. The more esteemed origin of LID in silicon is attributed to B–O defects and was discovered and electrically identified by Schmidt et al. [4,20]; they showed that the LID phenomenon depends on boron concentration, absent in gallium-doped and Fz-boron-doped silicon wafers.

Schmidt et al. [5] introduced a model where the fast diffusion of oxygen dimer (positively charged) activates defect formation. That captures the immobile substitutional boron atoms (negatively charged)

\* Corresponding author.

E-mail address: [salma.aouida@crten.rnrt.tn](mailto:salma.aouida@crten.rnrt.tn) (S. Aouida).

**Table 1**

Doping levels, resistivity, and average effective lifetime values of studied samples.

	[B] ( $10^{17} \text{cm}^{-3}$ )	[P] ( $10^{17} \text{cm}^{-3}$ )	$P_0 = [B] - [P]$ ( $10^{17} \text{cm}^{-3}$ )	Resistivity ( $\Omega \cdot \text{cm}$ )	Average of initial $\tau_{\text{eff}} (\mu\text{s})$
Sample A	2.80	1.60	1.20	0.35	2.3
Sample B	3.00	1.85	1.15	0.51	12
Sample E	4.15	5.30	-1.20	0.61	32

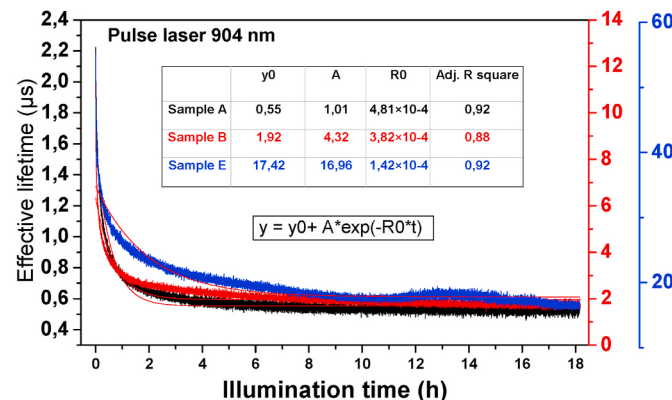


**Fig. 1.** (Color) Measured lifetime on the local excitation point versus time of the studied silicon samples,

Table inside: exponential fitting parameters

to form  $B_s-O_{2i}$  recombination centers; in such a situation, the concentration of the metastable boron-oxygen complex in crystalline silicon depends proportionally on the substitutional boron concentration and in a quadratic manner on the interstitial oxygen content. The model was prevailing for many years but was invalidated by Macdonald et al. [21] when they discovered that the degradation is controlled by the concentration of holes  $[p_0]$  instead of boron concentration  $[B]$ . In 2010, Voronkov and Falster [22] proposed a new degradation model in which degradation starts from a latent complex  $B_iO_2$  formed by an interstitial boron atom and an oxygen dimer. After carrier generation, a reconstruction of B-O complexes results in the production of recombination centers. This model is the first one that demonstrates the proportionality between defects concentration and holes concentration  $[p_0]$  in boron-phosphorus co-doped silicon. More recently, Vaqueiro-Contreras et al. [16], employing deep level transition spectroscopy and lifetime spectroscopy experiments, reveal the existence of a deep donor state in LID-deactivated boron-doped silicon wafer, which disappear progressively with LID activation. They conclude the deep boron-di-oxygenated donor state's conversion into a shallow acceptor under illumination [16]. The shallow acceptor state presents a trap-assisted Auger recombination centre.

The study of LID-related defects' kinetic formation or, more explicitly, B-O complexes reveals two degradation mechanisms [6,23–25]. For typical p-type silicon wafers, degradation occurs via a rapid initial decrease in minority carrier lifetime through rapidly fast-forming recombination centers (FRCs) within minutes, followed by slower decay on a timescale of several tens of hours to a few days due to slow-forming recombination centers (SRC). Most studies on p-type silicon show that the influence of the SRC on the device operation of the solar cell is more substantial than for the FRC. Therefore, the problematic degradation focuses mainly on SRC, while the influence of FRC is often neglected. However, recent work carried out in 2016 [26] has shown that the two latent  $B-O_2$  defects (the precursors of FRC and SRC)

are created during the cooling step of the silicon ingot, and their concentration is proportional to the boron concentration  $[B_i^+]$  and the squared oxygen concentration  $[O_{2i}]$ . In a recent contribution by Hallem et al. [27,28] and Kim et al. [29] suggested a theoretical model that describes the kinetics of degradation using a single recombination active defect. They suggest that the FRC activation is the fast activation of a defect precursor, while SRC is formed from a species that undergo a transition to this precursor first.

Besides, most previous works were focused on p-doped silicon (exclusively) with boron, while recently, the LID has been studied in both boron (p-type) and phosphorus (n-type) Cz-Si [30]. Results based on compensated p-type Cz-Si show that the compensation reduces the recombination strength of  $BO_{2i}$  complexes, and their concentration depends on the net doping (i.e.,  $[B]-[P]$ ). B atoms and P atoms form BP pairs [9,21,31], which minimizes the defect concentration since all boron may be compensated. Thus, the B-P-compensated n-Si can be affected by the LID, i.e., some  $BO_{2i}$  are formed, but their recombination activity is weaker than in p-Si, due to asymmetric electron and hole capture cross-sections.

In this work, we focus on compensated silicon wafers co-doped with boron and phosphorus. We examine the effect of the net-doping on the minority carrier lifetime and the activation of LID defect. Minority carrier lifetime mapping before and after sample illumination enables to estimate of the LID defect density. Mapping investigations show a Gaussian distribution of the LID defect density centered on the excitation point. The defect density decreases with the increase of phosphorus amount. A far as we know, it is the first time that a mapping of the LID defect density was reported, showing that LID defect diffuses through the sample. The LID defect diffusion process may be the origin of the observed slow defect generation.

## 2. Experiments

This study was carried out on highly doped silicon samples cut from wafers originating from the same monocrystalline Czochralski silicon (Cz-Si) ingot intentionally doped with boron (B) and phosphorus (P) atoms. During the crystallization step, the dopant impurities were progressively incorporated in the melt of the silicon bath. Their various segregation coefficients lead to vast resistivity values along the ingot [32,33]. Depending on the wafer position in the formed ingot, intrinsic, p-type, and n-type crystalline silicon wafers are formed. The concentrations of boron and phosphorus were determined by Glow-Discharge Mass Spectroscopy (GDMS) measurements [34,35]. The resistivity was measured with a four-probe system. Table 1 summarizes the properties of the studied samples. The interstitial oxygen concentration obtained by Fourier transformed infrared (FTIR) measurements is around  $8.5 \times 10^{17} \text{cm}^{-3}$ . The samples were double-sides passivated by hydrogenated silicon nitride ( $\text{SiN}_x:\text{H}$ ) coat using a plasma-enhanced chemical vapor deposition (PECVD) process to minimize surface recombination. A 200 °C/60 min dark annealing in a furnace tube quartz was used to annihilate the LID complexes and reach the initial annealed state before light treatment [12]. Effective lifetime measurements and mapping investigations were done using μPCD WT2000-VPN from Semilab in transient mode with 250 μm scan resolution. A lifetime mapping was performed on each sample before and after light treatment. The local defect activation was carried out using a pulsed laser excitation with a wavelength of 904 nm, power  $12 \times 10^{12}$  photons/pulse (~5.28E-4 nW/pulse), a pulse width 200 ns, and a spotlight of 1 mm<sup>2</sup>, which is the setup of microwave photoconductance decay. The penetration depth of this wavelength in silicon is about 30 μm. Simultaneously, the effective carrier lifetime ( $\tau_{\text{eff}}$ ) was measured using μPCD Semilab WT2000-VPN equipment. We focus mapping investigations on a circle centered in the excitation point with a diameter of 20 mm to eliminate the edge effect. We suppose that the activated defects are the well-known boron oxygen-related light-induced degradation (BO-LID) complex [36].

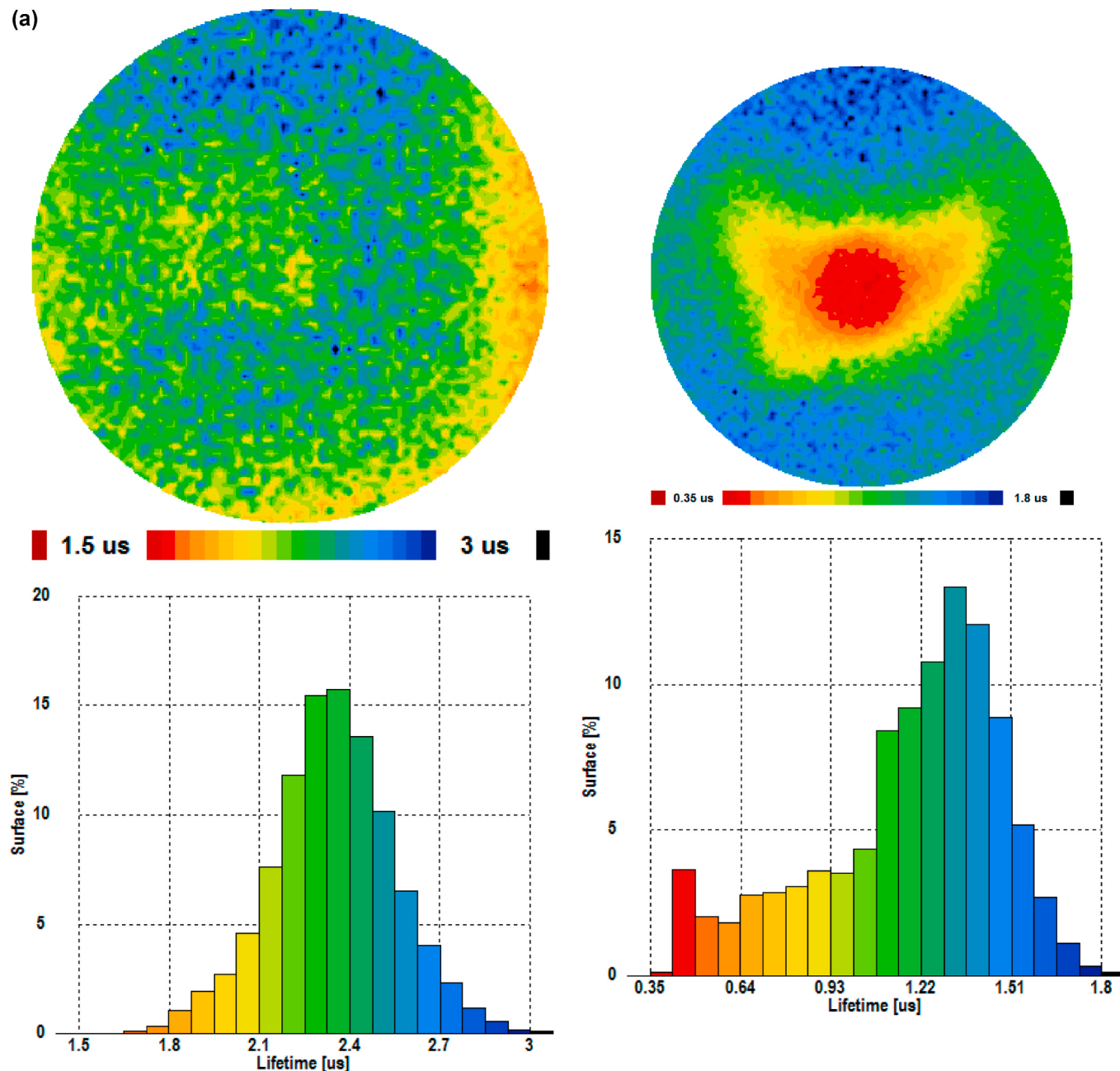


**Fig. 2.** Mapping and histogram minority carrier lifetime of sample A: (a) deactivation of LID defect after dark thermal treatment at 200 °C during 60 min (average lifetime = 2.3 μs), (b) after local LID activation (average lifetime = 1.3 μs)

### 3. Results and discussion

#### 3.1. Effect of phosphorus compensation on minority carrier lifetime of boron-doped silicon wafers

Co-doping silicon wafer by boron and phosphorus reduces the majority carrier concentration, which could be expressed by the co-doping amount or the net doping  $p_0 = [B] - [P]$  for p-type doping and  $n_0 = [N] - [B]$  for n-type doping.

Table 1 presents the average initial lifetime before LID activation of the studied samples and their net doping values. It is worth noting that samples studied in this work were taken from different height positions of the ingot and are labeled A, B (p-type doped), and E (n-type doped). For sample A, where  $p_0$  is about  $1.2 \times 10^{17} \text{ cm}^{-3}$ , the average lifetime value is 2.3 μs? This value increases to 12 μs for sample B, where

$p_0$  is equal to  $1.15 \times 10^{17} \text{ cm}^{-3}$ . The compensation induces an improvement in the value of the initial lifetime values, as shown in previous work [30]; this is explained by the compensation-induced reduction of the recombination strength of shallow energy levels and the Auger and radiative recombination rates [35]. Minority carrier lifetime illustrates the average time that the carrier remains free after its generation. This parameter depends on the carrier recombination process and gives valuable information about the low defect densities [37]. For surface-passivated silicon samples, like the studied ones, the main process is associated with the bulk Shockley-Read-Hall (SRH) recombination model [37,38]. This model is governed by traps having energy levels ( $E_t$ ) in the forbidden band. Generally, these traps are associated with doping species, metal impurities, and crystal defects. Boron is an acceptor element that gives rise to a shallow level in the vicinity of the valence band, having an energy of about  $E_A-E_V = 0.045 \text{ eV}$  [39]. The

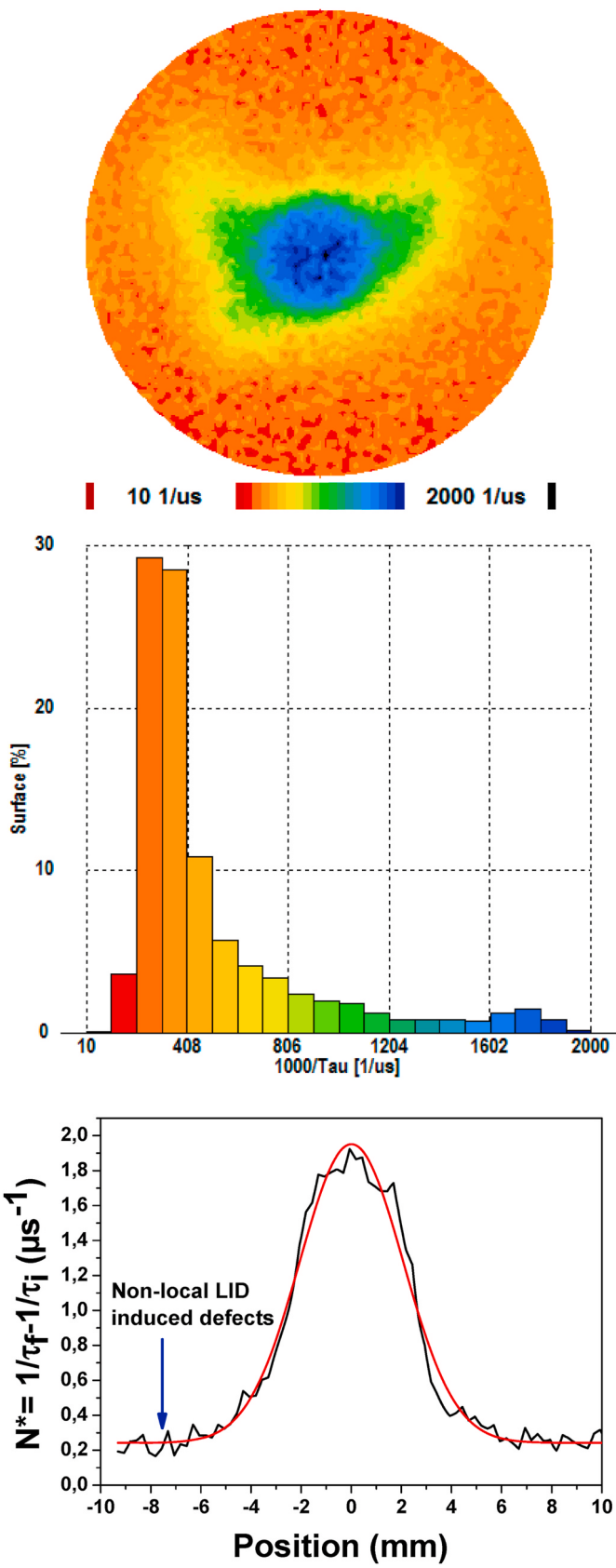


Fig. 3. Mapping, histogram, and a line scan of effective LID defects concentration  $N^*$  of sample A.

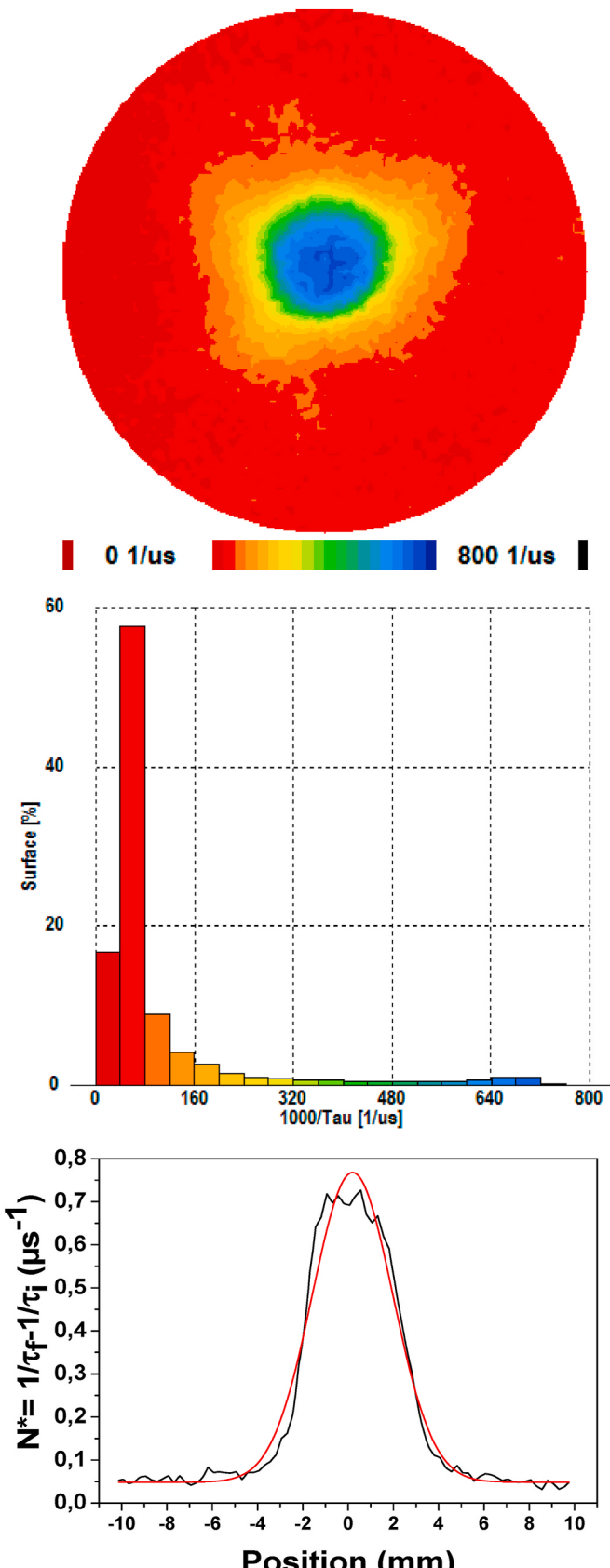
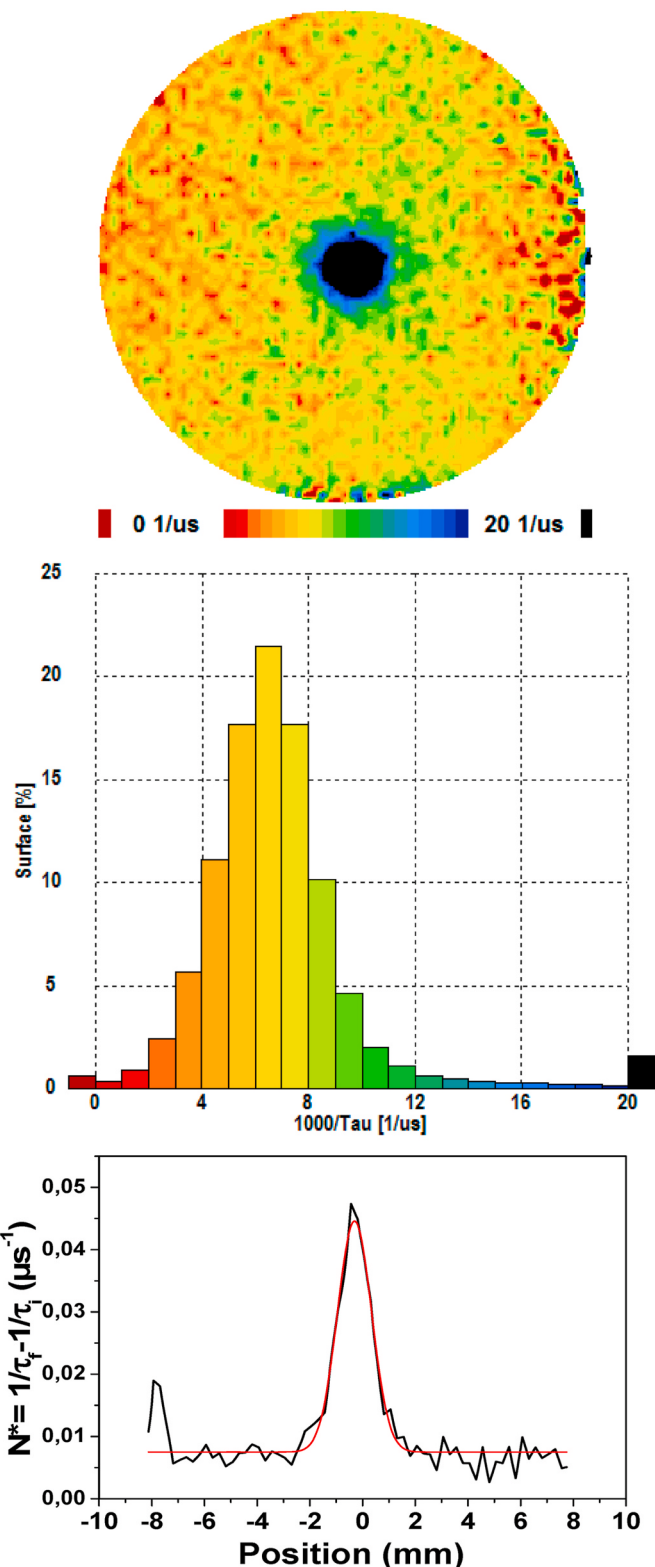
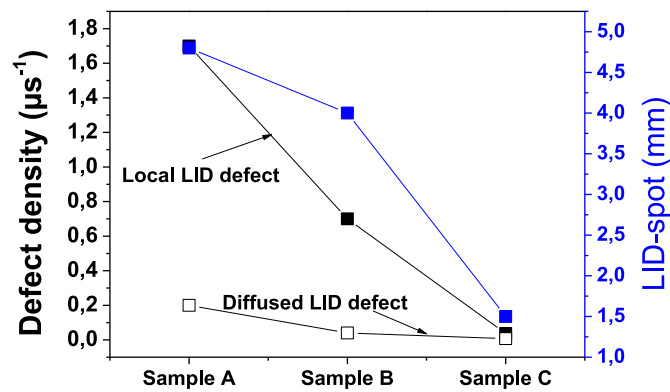


Fig. 4. Mapping, histogram, and a line scan of effective LID defects concentration  $N^*$  of sample B.



**Fig. 5.** Mapping, histogram, and a line scan of effective LID defects concentration  $N^*$  of sample E.

recombination occurs through excess holes in the valence band [37]. The strength of this process is sensitive to carrier concentration (i.e., doping amount). Highly doped materials ( $>10^{17} \text{ cm}^{-3}$ ) present low lifetimes [40]. The decrease of the majority carrier concentration increases the minority carrier lifetime. Phosphorus is a donor element giving a shallow level in the vicinity of the conduction band having an



**Fig. 6.** LID defects properties in highly co-doped silicon samples.

**Table 2**  
LID defects characteristics.

	$P_0 = [B] - [P]$ ( $10^{17} \text{ cm}^{-3}$ )	Local LID defect density ( $\mu\text{s}^{-1}$ )	LID-spot (mm)	Diffused LID defect density ( $\mu\text{s}^{-1}$ )
Sample A	1.2	1.7	4.8	0.2
Sample B	1.15	0.7	4	0.04
Sample E	-1.2	0.037	1.5	0.007

energy  $E_C - E_D = 0.045 \text{ eV}$  [39]. The co-doping reduces the excess holes by forming BP pairs in p-type samples, explaining the average of initial lifetime values between samples A and B (Table 1). For sample E, the average lifetime increases to  $32 \mu\text{s}$ . This is explained by the fact that holes became the minority carriers.

### 3.2. Local LID defects activation

LID defects in silicon samples can be activated through light exposure [2,21]. The local LID is activated via a pulsed laser excitation having a wavelength of  $904 \text{ nm}$  ( $12 \times 10^{12} \text{ photons/pulse}$ ) and a spotlight having a surface area of  $1 \text{ mm}^2$ . Fig. 1 presents the effective lifetime variation of the studied samples within excitation time, showing an exponential behavior. The exponential fit constant ( $R_0$ ) decreases with phosphorus amount increases (Fig. 1) and vary from  $4.81 \times 10^{-4} \text{ s}^{-1}$  in sample A to  $1.48 \times 10^{-4} \text{ s}^{-1}$  in sample E.

Fig. 2-a presents the lifetime mapping and surface histogram of the sample (A) after a total annihilation of LID defects by dark thermal treatment at  $200^\circ \text{C}$  for 60 min. The lifetime exhibits a Gaussian distribution in the  $1.5 \mu\text{s} - 3 \mu\text{s}$  range with an average value of  $2.3 \mu\text{s}$ . Fig. 2-b shows the lifetime mapping and surface histogram of sample (A) after local LID activation during 20 h; this process leads to the complete activation of LID defects at the excitation focal point (Fig. 1). It is worth noting the existence of two regions. The first corresponds to the excitation point (LID-spot) centre and is associated with low lifetime values between  $0.35 \mu\text{s}$  and  $0.6 \mu\text{s}$ . Outside the excitation spot, the second region corresponds to lifetime values of about  $1.8 \mu\text{s}$ , lesser than the initial average lifetime value ( $2.3 \mu\text{s}$ ). This exciting result suggests that the LID defect diffuses throughout the whole silicon sample.

To quantify the spatial distribution of LID defect, we convert lifetime mapping into the effective LID defects concentration ( $N^*$ ) mapping [41];  $N^*$  is defined as  $1/\tau_{fm} - 1/\tau_{im}$ , where  $\tau_{im}$  and  $\tau_{fm}$  are the initial and the final measured lifetime considered in the same sample position, respectively. Fig. 3 depicts the corresponding mapping, the surface histogram, and the diametric line scan.

LID defect concentration goes along a Gaussian distribution having a Full Width at Half Maximum (FWHM) of  $4.8 \text{ mm}$  and centered in the

excitation point where  $N^*$  is about  $1.9 \mu\text{s}^{-1}$ . Diffused defects labeled non-local LID defects diffuse throughout the silicon sample; for sample (A), they reach a concentration of  $0.2 \mu\text{s}^{-1}$  far away from the excitation point (Fig. 2). These values of LID defect density are relatively high compared with other studies [21]; this is due to the high doping level of the silicon samples ( $10^{17} \text{ cm}^{-3}$ ) that leads to amplification of the light effect.

### 3.3. Effect of phosphorus compensation on local LID activation

The same treatment and analysis were carried out on samples B and E; their corresponding mapping, surface histogram, and diametric line scan of LID defects concentration are shown in Figs. 4 and 5. The main properties of the formed LID defects in all samples are presented in Fig. 6 and summarized in Table 2. We notice that as  $p_0$  decreases from  $1.2 \times 10^{17} \text{ cm}^{-3}$  (sample A) to  $1.15 \times 10^{17} \text{ cm}^{-3}$  (sample B), the effective concentration ( $N^*$ ) of the local defect moves from  $1.9 \mu\text{s}^{-1}$  to  $0.7 \mu\text{s}^{-1}$ , indicating a decrease in LID defect activation; in this case, the effective concentration of non-local defects decreases from  $0.2 \mu\text{s}^{-1}$  to  $0.04 \mu\text{s}^{-1}$ , and the LID-spot slightly decreases from 4.7 mm to 4 mm (Table 2). The increase in P concentration (sample B) corresponds to a decrease in hole concentration, resulting in a low LID defect activation.

It is interesting to note that for the n-type co-doped silicon sample (Sample E), the local LID defect concentration value is about  $0.045 \mu\text{s}^{-1}$ , LID activation is relatively weak, the diffused non-local LID defects can be neglected (around  $0.007 \mu\text{s}^{-1}$ ), and the LID-spot is around 1.5 mm, quasi-equal to that of the laser spot. It is important to remember that in sample E, the boron concentration is  $4.15 \times 10^{17} \text{ cm}^{-3}$ , higher than samples A and B (Table 1). This result perfectly illustrates the effect of the hole concentration on the formation of LID defects. In fact, for the n-type silicon sample, the majority carriers are electrons, and the excess minority carrier 'holes' are located only in the vicinity of light excitation.

## 4. Discussion

The main of the obtained results is the diffusion of LID defects through the silicon sample. The nature of this diffusion is not easy to explain. However, considering that their origin is a latent state of B–O complexes or recombination-inactive precursors [42], which transform on shallow acceptor under illumination [16], we can suppose that firstly, the excess carrier generated by the laser pulse presents a spatial distribution in the silicon lattice [43] and activates the LID defects around the excitation point and presents the fast LID-process. The spatial distribution depends on the carrier diffusion length and does not exceed one mm from the generation point. With continuous laser light excitation, the transformed latent state interact with their neighbors and assure the activation of non-local LID defects, and leads to the slow LID-process. The increase of phosphorus amounts limits the formation of LID-BO defects; this is principally due to the formation of BP pairs. The boron phosphorus co-doping presents a solution to reduce the light-induced degradation in silicon solar cell. Other technical solutions could be adopted, such as p-type gallium doped [44] or n-type Phosphorus-doped silicon wafers [45].

## 5. Conclusion

We have studied the local activation of light-induced degradation (LID) defects on highly co-doped B–P silicon wafers. The minority carrier lifetime mapping before and after defects activation allows estimating the defect concentration around the excitation point. We found that the LID defect concentration follows a Gaussian distribution. LID defects were obtained on all regions of the silicon sample, which exhibits their diffusion from the excitation point. Phosphorus was found to reduce the activity of LID defects. It is worth noting that lasers are frequently used in engineering silicon-based devices and could activate LID defects; in such a case, deactivation treatments at low temperature

should be considered to ensure silicon device performance.

## Data availability statement

The data that support the findings of this study are available from the corresponding author upon reasonable request.

## Author statement

1. MARWA NAJJAR Acquisition, analysis, and interpretation of data.
  2. BECHIR DRIDI REZGUI Samples preparation and valuable discussion.
  3. MONGI BOUAICHA Valuable discussion and interpretation of data.
  4. OLIVIER PALAIS Samples preparation and valuable discussion.
  5. BRAHIM BESSAIS Final approval of the version to be published.
  6. SELMA AOUIDA Acquisition, analysis, and interpretation of data.
- Drafting the article.

## Declaration of competing interest

The authors declare that they have no known competing financial interests or personal relationships that could have appeared to influence the work reported in this paper.

## Acknowledgements

The authors would like to thanks the Tunisian Ministry of Higher Education and Scientific Research and The Japan International Cooperation Agency for their financial support.

## References

- [1] T. Ishii, A. Masuda, Annual degradation rates of recent crystalline silicon photovoltaic modules, *Prog. Photovoltaics Res. Appl.* 25 (2017) 953–967.
- [2] H. Fischer, Investigation of Photon and Thermal Changes in Silicon Solar Cells, Conference Record of the 10 IEEE Photovoltaic Specialists Conference, 1973.
- [3] J. Knobloch, S. Glunz, D. Biro, W. Warta, E. Schaffer, W. Wetling, Solar Cells with Efficiencies above 21% Processed from Czochralski Grown Silicon, Conference Record of the Twenty Fifth IEEE Photovoltaic Specialists Conference-1996, IEEE, 1996, pp. 405–408.
- [4] J. Schmidt, A.G. Aberle, R. Hezel, Investigation of Carrier Lifetime Instabilities in Cz-Grown Silicon, Conference Record of the Twenty Sixth IEEE Photovoltaic Specialists Conference-1997, IEEE, 1997, pp. 13–18.
- [5] J. Schmidt, Light-induced Degradation in Crystalline Silicon Solar Cells, Solid State Phenomena, *Trans Tech Publ.*, 2004, pp. 187–196.
- [6] H. Hashigami, M. Dhamrin, T. Saitoh, Characterization of the initial rapid decay on light-induced carrier lifetime and cell performance degradation of Czochralski-grown silicon, *Japanese Journal of Applied Physics Part 1-Regular Papers Brief Communications & Review Papers* 42 (2003) 2564–2568.
- [7] H. Hashigami, Y. Itakura, T. Saitoh, Effect of illumination conditions on Czochralski-grown silicon solar cell degradation, *J. Appl. Phys.* 93 (2003) 4240–4245.
- [8] K. Bothe, J. Schmidt, Electronically activated boron-oxygen-related recombination centers in crystalline silicon, *J. Appl. Phys.* 99 (2006) 11.
- [9] J. Geilker, W. Kwapis, S. Rein, Light-induced degradation in compensated p-and n-type Czochralski silicon wafers, *J. Appl. Phys.* 109 (2011), 053718.
- [10] V.V. Voronkov, R. Falster, Light-induced Boron-Oxygen Recombination Centres in Silicon: Understanding Their Formation and Elimination, Solid State Phenomena, *Trans Tech Publ.*, 2014, pp. 3–14.
- [11] M. Xie, C.R. Ren, L.M. Fu, X.D. Qiu, X.G. Yu, D.R. Yang, An industrial solution to light-induced degradation of crystalline silicon solar cells, *Front. Energy* 11 (2017) 67–71.
- [12] J. Schmidt, K. Bothe, V.V. Voronkov, R. Falster, Fast and slow stages of lifetime degradation by boron-oxygen centers in crystalline silicon, *Physica Status Solidi B-Basic Solid State Physics* (2020) 257.
- [13] M. Winter, S. Bordihn, R. Peibst, R. Brendel, J. Schmidt, Degradation and regeneration of n+-doped poly-Si surface passivation on p-type and n-type Cz-Si under illumination and dark annealing, *IEEE Journal of Photovoltaics* 10 (2020) 423–430.
- [14] Z. Yao, D. Zhang, J. Wu, F. Jiang, G. Xing, X. Su, Evolution of LeTID defects in industrial multi-crystalline silicon wafers under laser illumination-Dependency of wafer position in brick and temperature, *Sol. Energy Mater. Sol. Cell.* 218 (2020) 110735.
- [15] J. Adey, R. Jones, D. Palmer, P. Briddon, S. Öberg, Degradation of boron-doped Czochralski-grown silicon solar cells, *Phys. Rev. Lett.* 93 (2004), 055504.

- [16] M. Vaqueiro-Contreras, V.P. Markevich, J. Coutinho, P. Santos, I.F. Crowe, M. P. Halsall, I. Hawkins, S.B. Lastovskii, L.I. Murin, A.R. Peaker, Identification of the mechanism responsible for the boron oxygen light-induced degradation in silicon photovoltaic cells, *J. Appl. Phys.* 125 (2019) 185704.
- [17] H.W.B. V. G. Weizer, J. D. Broder, R. E. Hart, and J. H. Lamneck, Photodegradation Effects in Terrestrial Silicon Solar Cells.
- [18] J. Corbett, A. Jaworowski, R. Kleinhenz, C. Pierce, N. Wilsey, Photodegradation in silicon, *Sol. Cell.* 2 (1980) 11–22.
- [19] S. Glunz, S. Rein, J. Lee, W. Warta, Minority carrier lifetime degradation in boron-doped Czochralski silicon, *J. Appl. Phys.* 90 (2001) 2397–2404.
- [20] J. Schmidt, A. Cuevas, Electronic properties of light-induced recombination centers in boron-doped Czochralski silicon, *J. Appl. Phys.* 86 (1999) 3175–3180.
- [21] D. Macdonald, F. Rougier, A. Cuevas, B. Lim, J. Schmidt, M. Di Sabatino, L. Geerligs, Light-induced boron-oxygen defect generation in compensated p-type Czochralski silicon, *J. Appl. Phys.* 105 (2009), 093704.
- [22] V.V. Voronkov, R. Falster, Latent complexes of interstitial boron and oxygen dimers as a reason for degradation of silicon-based solar cells, *J. Appl. Phys.* 107 (2010), 053509.
- [23] K. Bothe, J. Schmidt, Fast-forming boron-oxygen-related recombination center in crystalline silicon, *Appl. Phys. Lett.* 87 (2005) 3.
- [24] K. Bothe, R. Hezel, J. Schmidt, Recombination-enhanced formation of the metastable boron-oxygen complex in crystalline silicon, *Appl. Phys. Lett.* 83 (2003) 1125–1127.
- [25] A. Graf, A. Herguth, G. Hahn, Investigation on the dependence of degradation rate on hole concentration during boron-oxygen related light-induced degradation in crystalline silicon, *AIP Adv.* 8 (2018) 7.
- [26] V. Voronkov, R. Falster, Permanent deactivation of boron-oxygen recombination centres in silicon, *Phys. Status Solidi* 253 (2016) 1721–1728.
- [27] B. Hallam, M. Abbott, T. Naeiland, S. Wenham, Fast and slow lifetime degradation in boron-doped Czochralski silicon described by a single defect, *Phys. Status Solidi Rapid Res. Lett.* 10 (2016) 520–524.
- [28] B. Hallam, M. Kim, M. Abbott, N. Nampalli, T. Naeiland, B. Stefani, S. Wenham, Recent insights into boron-oxygen related degradation: evidence of a single defect, *Sol. Energy Mater. Sol. Cell.* 173 (2017) 25–32.
- [29] M. Kim, M. Abbott, N. Nampalli, S. Wenham, B. Stefani, B. Hallam, Modulating the extent of fast and slow boron-oxygen related degradation in Czochralski silicon by thermal annealing: evidence of a single defect, *J. Appl. Phys.* 121 (2017), 053106.
- [30] S. Dubois, N. Enjalbert, J. Garandet, Effects of the compensation level on the carrier lifetime of crystalline silicon, *Appl. Phys. Lett.* 93 (2008), 032114.
- [31] B. Lim, F. Rougier, D. Macdonald, K. Bothe, J. Schmidt, Generation and annihilation of boron–oxygen-related recombination centers in compensated p-and n-type silicon, *J. Appl. Phys.* 108 (2010) 103722.
- [32] Z. Liu, T. Carlberg, A model for dopant concentration in Czochralski silicon melts, *J. Electrochem. Soc.* 140 (1993) 2052.
- [33] H. Kodera, Diffusion coefficients of impurities in silicon melt, *Jpn. J. Appl. Phys.* 2 (1963) 212.
- [34] B.D. Rezgui, J. Veirman, S. Dubois, O. Palais, Study of donor–acceptor pair luminescence in highly doped and compensated Cz silicon, *Phys. Status Solidi* 209 (2012) 1917–1920.
- [35] J. Veirman, S. Dubois, N. Enjalbert, J.-P. Garandet, M. Lemiti, Electronic properties of highly-doped and compensated solar-grade silicon wafers and solar cells, *J. Appl. Phys.* 109 (2011) 103711.
- [36] J. Schmidt, K. Bothe, Structure and transformation of the metastable boron-and oxygen-related defect center in crystalline silicon, *Phys. Rev. B* 69 (2004), 024107.
- [37] D.K. Schroder, Carrier lifetimes in silicon, *IEEE Trans. Electron. Dev.* 44 (1997) 160–170.
- [38] W. Shockley, W.T. Read, Statistics of the recombinations of holes and electrons, *Phys. Rev.* 87 (1952) 835–842.
- [39] G.L. Pearson, J. Bardeen, Electrical properties of pure silicon and silicon alloys containing boron and phosphorus, *Phys. Rev.* 75 (1949) 865.
- [40] P. Altermatt, A. Schenk, G. Heiser, A simulation model for the density of states and for incomplete ionization in crystalline silicon. I. Establishing the model in Si: P, *J. Appl. Phys.* 100 (2006) 113715.
- [41] D.W. Palmer, K. Bothe, J. Schmidt, Kinetics of the electronically stimulated formation of a boron–oxygen complex in crystalline silicon, *Phys. Rev. B* 76 (2007), 035210.
- [42] T.H. Fung, M. Kim, D. Chen, C.E. Chan, B.J. Hallam, R. Chen, D.N. Payne, A. Ciesla, S.R. Wenham, M.D. Abbott, A four-state kinetic model for the carrier-induced degradation in multicrystalline silicon: introducing the reservoir state, *Sol. Energy Mater. Sol. Cell.* 184 (2018) 48–56.
- [43] K.L. Luke, L.J. Cheng, Analysis of the interaction of a laser pulse with a silicon wafer: determination of bulk lifetime and surface recombination velocity, *J. Appl. Phys.* 61 (1987) 2282–2293.
- [44] N.E. Grant, J.R. Scowcroft, A.I. Pointon, M. Al-Amin, P.P. Altermatt, J.D. Murphy, Lifetime instabilities in gallium doped monocrystalline PERC silicon solar cells, *Sol. Energy Mater. Sol. Cell.* 206 (2020) 110299.
- [45] S.H. Lee, Advancements in n-type base crystalline silicon solar cells and their emergence in the photovoltaic industry, *Sci. World J.* (2013) 2013.